

# MESH CONVERGENCE OF MOVING CONTACT LINES IN VOF SIMULATIONS

A. Guion<sup>\*1</sup>, J. Buongiorno<sup>1</sup>, S. Afkhami<sup>2</sup>, and S. Zaleski<sup>3</sup>

<sup>1</sup>*Massachusetts Institute of Technology, Cambridge, MA, USA*

<sup>2</sup>*New Jersey Institute of Technology, Newark, NJ, USA*

<sup>3</sup>*Institut Jean Le Rond d'Alembert, UPMC & CNRS-UMR 7190, Paris, FRANCE*

*Summary* The numerical simulation of moving contact lines is complicated by the stress singularity at the contact point, which prevents results from converging in a standard way. The objective of this work is to achieve mesh convergence of moving contact line results in VOF simulations, and to assess the applicability for a wide range of capillary numbers of the numerical model proposed by Afkhami et al. [1]. Based on fundamental hydrodynamics, the numerical model serves as a new boundary condition that adapts the microscopic contact angle as the mesh is refined, eliminating the stress singularity at the contact line. Systematic computations are performed to obtain convergence of the macroscopic interface shape near the moving contact line at a solid plate withdrawing from a fluid pool.

## INTRODUCTION

Contact line motion has been studied in the limit of small capillary numbers, when capillary forces dominate. Cox [2] and others have used matched asymptotic expansions to relate the microscopic contact angle ( $\theta_m$ ) with the macroscopic contact angle ( $\theta_w$ ) of the interface relative to the solid, respectively near the moving contact line (distance  $r_{in}$ ) and away from the moving contact line (distance  $r_{out}$ ,  $r_{out} \gg r_{in}$ ). An approximation of this asymptotic matching [3] has been used to obtain a contact angle boundary condition as a function of mesh size [1], in order to achieve mesh convergence in VOF simulations of moving contact lines. Same macroscopic contact line configurations were obtained for different microscopic mesh sizes, in the simulation of a partially wetting and withdrawing plate from a liquid reservoir at a small capillary number  $\text{Ca} = 0.03$ .

## NUMERICAL METHODS

We use the open-source code Gerris to solve the incompressible, variable-density, Navier-Stokes equations with surface tension [4]. The volume fraction  $c$  of the first fluid ( $\rho_1, \mu_1$ ) is used to define density  $\rho \equiv c\rho_1 + (1 - c)\rho_2$  and viscosity  $\mu \equiv c\mu_1 + (1 - c)\mu_2$ , where ( $\rho_2, \mu_2$ ) are properties of the second fluid. A time-splitting projection method is used, and requires an iterative solution procedure. Space is discretized using quad tree partitioning. A Volume Of Fluid (VOF) scheme is used to track (advect and reconstruct) the interface.

## SIMULATION PROPERTIES

Consider a solid plate withdrawing at a velocity  $U$  from a square fluid pool of length  $L/l_c = 20$ , with  $l_c$  the capillary length:  $l_c = \sqrt{\sigma/\rho g}$ . The density ratio is set to 20, and viscosity ratio to 1. The interface between the two fluids is initially flat at height  $h_0/l_c = 7$ . No slip and a fixed microscopic contact angle  $\theta_m$  are prescribed at the wall. The contact line motion along the wall evolves to a stationary state for  $\tau \gg 1$ , with  $\tau = (U \cdot t)/l_c$ . Systematic computations are performed to span a wide range of contact angles  $\theta$ , Capillary numbers, and cell sizes at the contact line  $dx/l_c$ , as detailed in Table 1.

Mesh refinement is increased at the interface, in the vicinity of the contact line, and where the error on velocity is the highest. In Figure 1, the inner region (in blue) in the vicinity of the contact line is sufficiently refined to resolve small scale effects, up to the inflexion point of the interface, where its curvature becomes positive (in red). The computational domain shown in Figure 1 is truncated: a static microscopic contact angle, and no-slip, are prescribed at the left boundary of the domain; symmetry on the right boundary of the domain (at  $x/l_c = 20$ ); top and bottom boundaries allow flow in and out of the domain.

Table 1: Simulation parameters

Contact angle $\theta$ [°]	Capillary number $\text{Ca}$ [—]	Minimum cell size $dx/l_c$ [—]
50, 55, 60, 65, 70, 75, 80, 85, 90	0.01, 0.02, 0.04, 0.08, 0.16	1/16, 1/32, 1/64, 1/128, 1/256

\*Corresponding author. Email: aguion@mit.edu

## RESULTS

In the wide range of capillary numbers simulated, we both observe the development of a steady meniscus at the partially wetting wall (see blue, black and magenta profiles in Figure 2 (a)), and the Landau-Levich transition at higher values of  $Ca$ , where the liquid meniscus is entrained and leads to the formation of a thin film at the wall (red profiles, Figure 2 (a)). The position of the meniscus once it has reached its stationary state, e.g. when all forces are in equilibrium, is reported for all  $Ca$ ,  $\theta$  and  $dx/l_c$  (see Figure 2 (b)). This work systematically quantifies the effect of mesh refinement and contact angle on the final position of the contact line, for a range of capillary numbers below the Landau-Levich transition threshold. It is then possible to adjust the microscopic contact angle a priori with mesh refinement to obtain convergence of the results (see Figure 2 (c)).

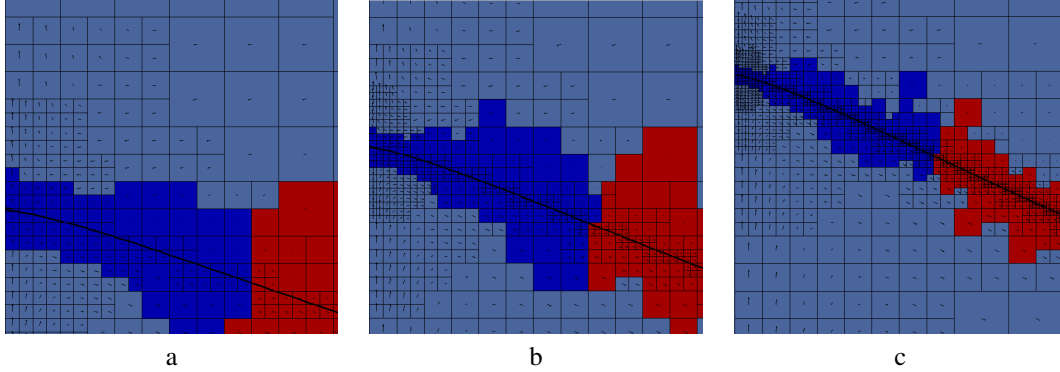


Figure 1: Stationary shape and position of the contact line (black line), for the same window of observation, but different minimum cell sizes  $dx/l_c = 1/16$  (a),  $1/32$  (b),  $1/64$  (c). The curvature is negative (blue) then positive (red).

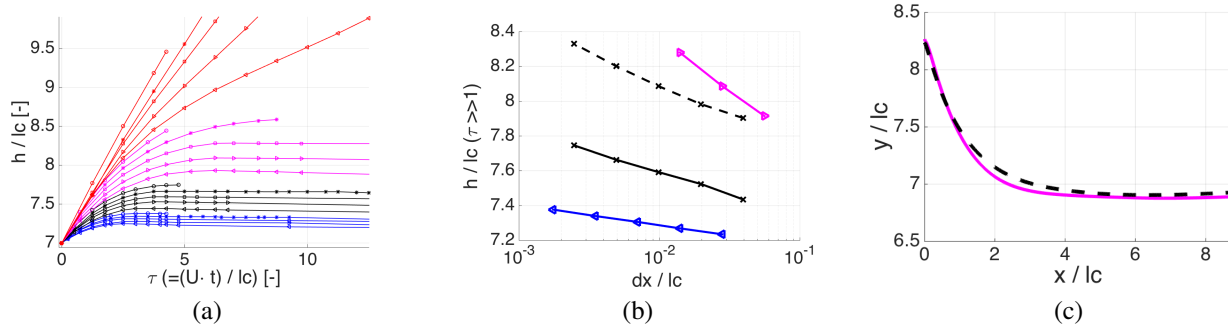


Figure 2: (a) Contact line height as function of time for  $\theta_m = 90^\circ$ ,  $Ca \in \{10^{-2}$  (blue),  $2 \cdot 10^{-2}$  (black),  $4 \cdot 10^{-2}$  (magenta),  $8 \cdot 10^{-2}$  (red) $\}$ , and  $dx/l_c \in \{1/16$  ( $\triangleleft$ ),  $1/32$  ( $\triangleright$ ),  $1/64$  ( $\square$ ),  $1/128$  ( $\star$ ),  $1/256$  ( $\circ$ ) $\}$ . (b) Stationary heights of the contact line as function of cell size. Dashed line for  $\theta_m = 70^\circ$ . (c) Stationary contact line shapes for  $(dx/l_c, \theta) \in \{(1/64, 70^\circ), (1/32, 90^\circ)\}$

## CONCLUSIONS

The numerical model proposed in [1] is applied to a wider range of capillary numbers. The systematic adjustment of microscopic contact angles with mesh refinements makes it possible to refine the grid arbitrarily, while still eliminating the stress singularity at the contact line and obtaining mesh convergence of the results.

### References

- [1] S. Afkhami, S. Zaleski, M. Bussmann: A mesh-dependent model for applying dynamic contact angles to vof simulations. J. Comp. Phys., 228:5370-5389, 2009.
- [2] R.G. Cox, The dynamics of the spreading of liquids on a solid surface. Part 1. Viscous flow, J. Fluid Mech., 168:169-194, 1986
- [3] P. Sheng, M. Zhou, Immiscible-fluid displacement: contact-line dynamics and the velocity-dependent capillary pressure, Phys. Rev. A 45 (8):5694-5708, 1992
- [4] S. Popinet: An accurate adaptive solver for surface-tension-driven interfacial flows J. Comp. Phys., 228:5838-5866, 2009